Journal of Hydroscience and Hydraulic Engineering
Vol. 17, No.2 November, 1999, 87-96

3-D COMPUTATIONS OF COMPOUND OPEN CHANNEL FLOWS WITH HORIZONTAL VORTICES AND SECONDARY CURRENTS BY USING NON-LINEAR k-ε MODEL

by

T. HOSODA
Department of Civil Engineering, Kyoto University, Kyoto, Japan

T. SAKURAI
Public Works Research Institute, Ministry of Construction, Tsukuba, Japan

I. KIMURA
Faculty of Environmental and Information Sciences, Yokkaichi University, Yokkaichi, Japan

and

Y. MURAMOTO
Department of Civil Engineering, Osaka College of Technology, Osaka, Japan

SYNOPSIS

A non-linear k-ε model is applied to 3-D computations of unsteady flows in compound open channels with horizontal vortices generated by the shear instability and the secondary currents of the second kind. It is pointed out that the typical flow features such as the horizontal vortices and the secondary currents can be simulated numerically by using the non-linear kε model including the effect of the strain parameter on the eddy viscosity, though further refinements of the model are needed to reproduce the 3-D flow structures more precisely. In view of the model refinement, it is tested to include the cubic terms in the constitutive equations of the non-linear k-ε model on trial. It is shown that the calculated flow patterns of the secondary currents are improved qualitatively compared with the previous experimental studies, though the effect of cubic terms on the Reynolds stresses and the numerical values of model constants should be examined in detail.

INTRODUCTION

Flows in compound open channels are characterized by the steady secondary currents of the second kind induced by the anisotropy of the Reynolds stresses and the unsteady large-scale horizontal vortices generated by the shear layer instability, which are observed at a junction of the main channel and the flood plain (Tamai, Asaeda and Ikeda(17)). It is known that the horizontal vortices increase the resistance to flow due to the large momentum transfer through a junction (Fukuoka and Fujita(2)).

As for the secondary currents in the rectangular and compound open channels, the applicability of the algebraic Reynolds stress models have been verified by Naot and Rodi(12), Naot, Nezu and Nakagawa(13) and Sugiyama, Akiyama and Matsubara(16), considering the existence of water surfaces. On the other hand, it was shown that the horizontal vortices with long periods generated by the shear instability can be simulated by the two-layered depth averaged model (9).

The computational model to simulate the 3-D unsteady flow structures with both the secondary currents and the horizontal vortices is developed in this paper. Since the observed periods of horizontal

vortices are much longer than the turbulence time scale, Reynolds averaged turbulence models should be applicable to the generation of vortices by the shear instability due to transverse velocity distributions. A non-linear k-ε model seems to be applicable to the secondary currents of the second kind in open channel flows if the existence of the water surface is taken into account, because the model is equivalent to the algebraic Reynolds stress model as shown by Pope (15) and Gatski and Speziale (3). Pezzinga(14) verified the applicability of the non-linear k-ε model with the quadratic terms and the Oldroid derivative of strain-rate tensors to the steady flow patterns of the secondary currents in a compound channel. Lin and Shiono(11) also calculated the 3-D steady flows in a compound channel by using the non-linear k-ε model with a part of the quadratic terms.

It was also shown that the non-linear k-ε model is also applicable to the flow induced by shear instability (6), if the relation between the proportional constant, C_μ, and the strain parameter, S, is considered to evaluate the Reynolds stresses. In the study, the functional form proposed by Kato and Launder (8) was used as the relation between C_μ and S, tuning the model constants. It was shown that the generation of shear instability depends on the model constants of the relation (6).

In this paper, the numerical model based on a non-linear k-ε model is tested for the calculation of flows in a compound open channel, and the model performances such as 3-D flow structures near a vortex and secondary currents are examined.

BASIC EQUATIONS AND NUMERICAL MODEL

The basic equations are composed of the continuity equation, the momentum equations, and the k-ε equations, described below:

[Continuity equation]

$$\frac{\partial U_i}{\partial x_i} = 0 \tag{1}$$

[Momentum equations]

$$\frac{\partial U_i}{\partial t} + \frac{\partial U_j U_i}{\partial x_j} = g_i - \frac{1}{\rho}\frac{\partial p}{\partial x_i} + \frac{\partial - \overline{u_i u_j}}{\partial x_j} + \nu \frac{\partial^2 U_i}{\partial x_j^2} \tag{2}$$

[k-ε equation]

$$\frac{\partial k}{\partial t} + \frac{\partial k U_j}{\partial x_j} = -\overline{u_i u_j}\frac{\partial U_i}{\partial x_j} - \varepsilon + \frac{\partial}{\partial x_j}\left\{\left(\frac{D}{\sigma_k} + \nu\right)\frac{\partial k}{\partial x_j}\right\} \tag{3}$$

$$\frac{\partial \varepsilon}{\partial t} + \frac{\partial \varepsilon U_j}{\partial x_j} = -C_{\varepsilon 1}\overline{u_i u_j}\frac{\partial U_i}{\partial x_j} - C_{\varepsilon 2}\frac{\varepsilon^2}{k} + \frac{\partial}{\partial x_j}\left\{\left(\frac{D}{\sigma_\varepsilon} + \nu\right)\frac{\partial \varepsilon}{\partial x_j}\right\} \tag{4}$$

where x_i: spatial coordinates, t: time, U_i: components of time averaged velocity vectors, u_i: components of turbulent velocity vectors, p: pressure, ρ: density of fluid, k: turbulent energy, ε: turbulent energy dissipation rate, ν: molecular dynamic viscosity, σ_k: model constant(=1.0) and σ_ε: model constant(=1.3).

The Reynolds stresses are evaluated by the following equations based on the non-linear k-ε model with the quadratic terms proposed by Yoshizawa (19), which is equivalent to the expression by Pope(15) and Gatski and Spaziale (3). The relation between the non-linear k-ε model and the algebraic stress model was made clear by Pope (15) and Gatski and Spaziale (3).

$$-\overline{u_i u_j} = DS_{ij} - \frac{2}{3}k\delta_{ij} - \frac{k}{\varepsilon}D\sum_{\beta=1}^{3}C_\beta\left(S_{\beta ij} - \frac{1}{3}S_{\beta\alpha\alpha}\delta_{ij}\right);\ D = C_\mu\frac{k^2}{\varepsilon} \tag{5}$$

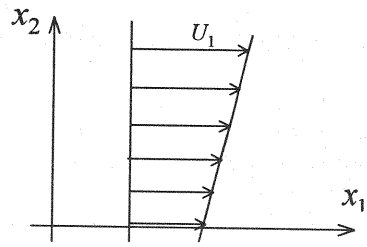

Fig.1 Schematic illustration of simple shear flow

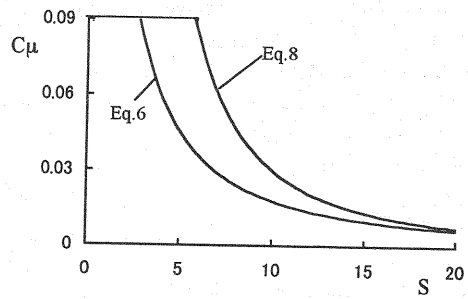

Fig.2 Relation between $C\mu$ and S

$$S_{ij}=\frac{\partial U_i}{\partial x_j}+\frac{\partial U_j}{\partial x_i};\quad S_{1ij}=\frac{\partial U_i}{\partial x_r}\frac{\partial U_j}{\partial x_r};\quad S_{2ij}=\frac{1}{2}\left(\frac{\partial U_r}{\partial x_i}\frac{\partial U_j}{\partial x_r}+\frac{\partial U_r}{\partial x_j}\frac{\partial U_i}{\partial x_r}\right);\quad S_{3ij}=\frac{\partial U_r}{\partial x_i}\frac{\partial U_r}{\partial x_j}$$

Since it was pointed out that the vortices generated by the shear instability cannot be simulated without including the effect of the strain parameter (Hosoda et al. (6)), the relation between C_μ and the strain parameter, S, is also included in the model using the following functional form (Kato and Launder (8)).

$$S=\frac{k}{\varepsilon}\sqrt{\frac{1}{2}\left(\frac{\partial U_i}{\partial x_j}+\frac{\partial U_j}{\partial x_i}\right)^2};\quad C_\mu=\min\left[0.09,\frac{A_2}{1+A_1(\min[20,S])^{1.5}}\right] \tag{6}$$

For the sake of simplicity, the rotation parameter is not considered in the model. Because the strain parameter is equivalent to the rotation parameter, in case that the instability is induced by the transverse velocity distribution like a simple shear flow, which is uniform in the stream-wise direction.

CONSIDERATIONS OF RELATION BETWEEN C_μ AND S

The ranges of model constants to satisfy the realizability conditions for various simple flow patterns such as a simple shear flow, which guarantees the positive turbulent intensities, were considered by Fu, Rung and Thiele (1). In the case of a simple shear flow shown in Fig.1, applying the same procedures to Eq.5, the constraint for C_μ itself can be derived as follows:

The turbulent intensities in the transverse direction (x_2) are reduced to Eq.7.

$$\frac{\overline{u_2u_2}}{k}=\frac{2}{3}+C_\mu\frac{2C_3-C_1}{3}S^2,\ S=\frac{k}{\varepsilon}\left|\frac{\partial U_1}{\partial x_2}\right| \tag{7}$$

The condition of positive turbulent intensities requires the constraint denoted by Eq.8.

$$C_\mu<\frac{2}{(C_1-2C_3)S^2} \tag{8}$$

Eq.8 with the model constants, $C_1=0.4, C_3=-0.13$ shown in Fig.2 indicates that Eq.6 with $A_1=0.5, A_2=0.3$ used in the computations satisfy the realizability condition for a simple shear flow.

OUTLINE OF CALCULATIONS

The common finite volume method is used with the iterative procedure to calculate the pressure (Hirt and Cook (4)). The QUICK scheme is utilized as the finite difference form of the convection term in the momentum and k-ε equations. The free surface elevation is calculated by solving the continuity equation integrated over the fixed control volume at the surface layer.

The 3-D unsteady flow analysis was carried out under the conditions of the laboratory tests by Ikeda et al(7). The cross section of the flume (the bottom slope, 1/1000) is shown in Fig.3. The flow domain is divided into the 10(depth-wise direction) , 40(transverse direction) and 200(stream-wise direction, $\Delta x = 4(cm)$) control volumes as shown in Fig.3. The time increment, Δt , is 0.002(sec).

The model constants are listed in the Table 1. The constants, $C_1 \sim C_3$, are adjusted examining the calculated flow patterns of the secondary currents, though the calculated results are not compatible with the qualitative characteristics of the previous laboratory tests yet. A_1 and A_2 are tuned checking on the generation of horizontal vortices at the junction, because the instability could not be detected by using the original constants of Kato·Launder model (8).

The relation between the proportional constant, C_μ , and the strain parameter, S , is shown in Fig.2. When the wall function method is applied as the wall boundary condition, the numerical value of S evaluated by the wall function is $1/\sqrt{2 \cdot 0.09} \approx 2.36$. In this case, it is indicated that the non-linear k-ε model does not change the near wall boundary condition, because $C_\mu = 0.09$ *at* $S \approx 2.36$ as shown in Fig.2.

To consider the rapid attenuation of turbulent intensities in the depth-wise direction near the water surface, the following dumping function, f_s , is multiplied by the eddy viscosity (5) and the turbulent intensity in the direction perpendicular to the water surface is also forced to be zero in the control volume of water surface layer (16). The turbulent dissipation rate at the water surface layer, ε_s is evaluated by the following formula (16).

$$f_s = 1 - \exp(-B\frac{(h-y)\varepsilon_s}{k_s^{3/2}}), \quad \varepsilon_s = \frac{C_{\mu 0}^{3/4} k_s^{3/2}}{0.4\Delta y_s}, \ (B = 10,\ C_{\mu 0} = 0.09) \tag{9}$$

where h: depth and sub-s indicates the value at the surface layer.

CONSIDERATIONS OF CALCULATED RESULTS

The plan views of flow patterns (t=130sec.) observed in the moving coordinate with the constant velocity, 15(cm/s), are shown in Fig.4. The spatial development of the large scale horizontal vortices generated by shear instability can be observed from the middle part to the downstream-end of the flume. Fig.5 shows the same flow patterns in the downstream part at t=90(sec.). Since the lengths between these vortices at different two times are the same, the spatial equilibrium state seems to be realized in the downstream part of the flume.

The flow patterns at several cross sections in the transverse direction indicated in Fig.4 are shown in Fig.6. The secondary currents of the second kind and the flows induced by the horizontal vortices can be observed in these cross sections. The strong upward flow is generated in the central part of a horizontal vortex as seen in Fig.6(c)

The calculated three dimensional flow structure is in good agreement with the schematic illustration of flow shown in Fig.7, depicted by Ikeda et al. (7) using the flow visualization.

Fig.8 shows the depth variations along the junction. The positions of minimum depth almost coincide with centers of vortices. The calculated length between vortices, 60(cm), is a little shorter than the observed length, 73.3(cm). The calculated amplitude of depth variations, 0.3(mm) is also smaller than the observed one(0.4mm).

Table 1 Model constants used for the calculation

$C_{\varepsilon 1}$	$C_{\varepsilon 2}$	σ_k	σ_ε	C_1	C_2	C_3	A_1	A_2
1.44	1.92	1.0	1.3	0.4	0	−0.13	0.5	0.3

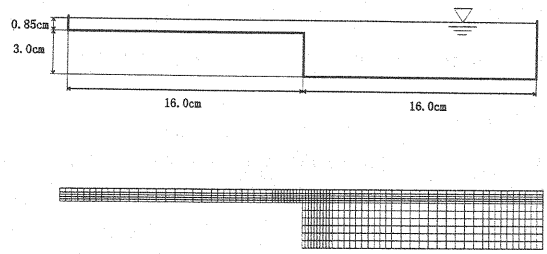

Fig.3 Cross-section of flume and grid system

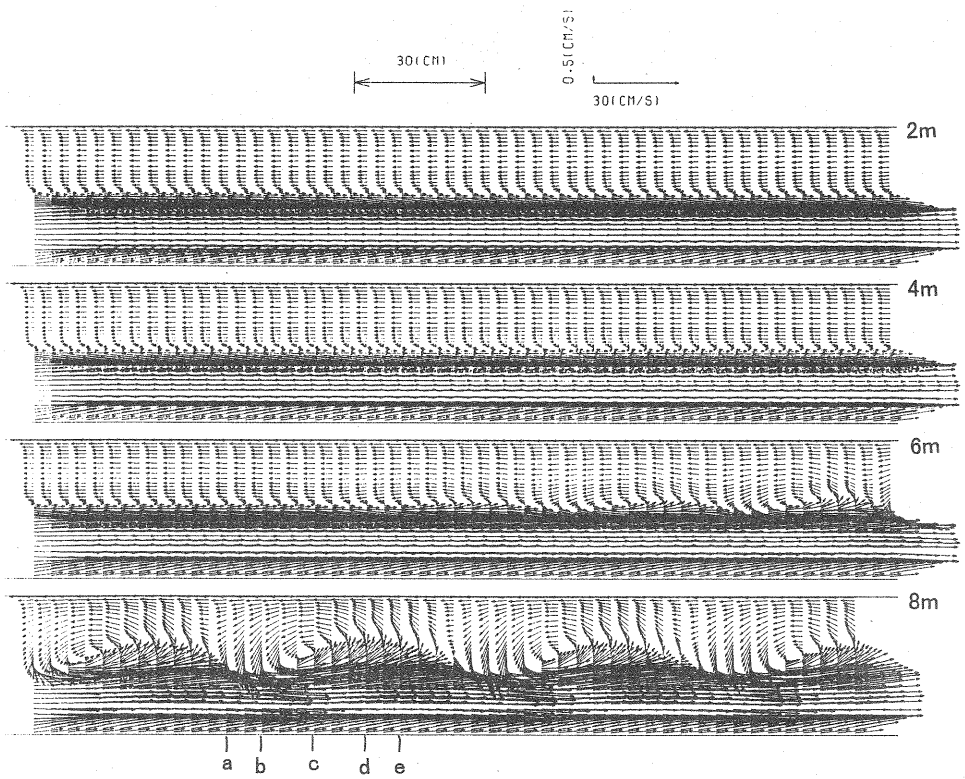

Fig.4 Plan view of flow patterns (the 3rd layer from the surface layer, t=130(sec))

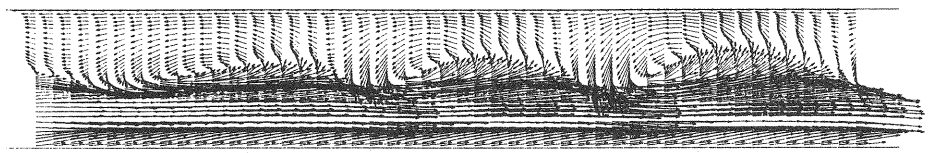

Fig.5 Plan view of flow patterns
(the 3rd layer from the surface layer between 6m and 8m, t=90(sec))

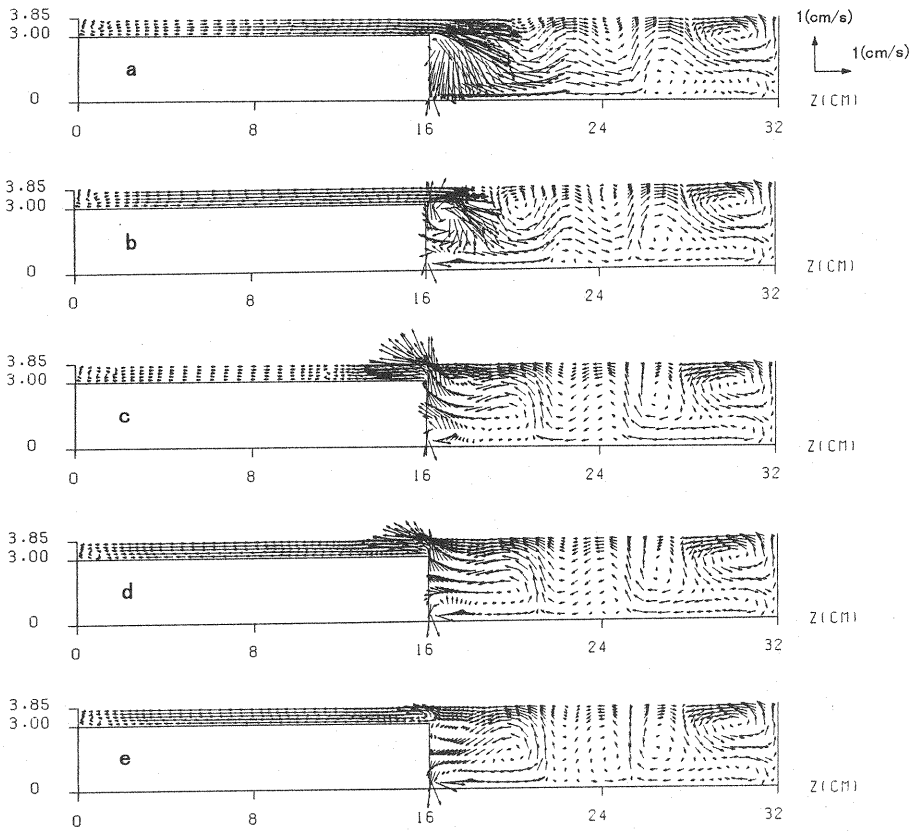

Fig.6 Flow patterns at several cross sections
(Positions of cross sections are indicated in Fig.4.)

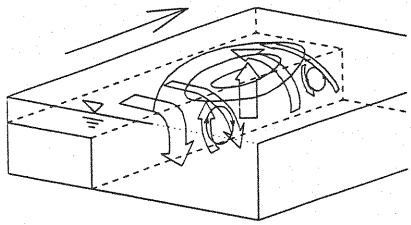

Fig.7 Schematic illustration of 3-D flow structure by Ikeda et al(7)

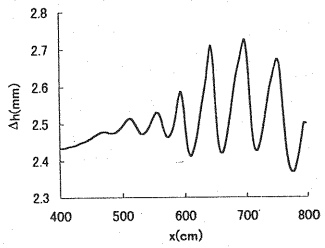

Fig.8 Depth variations along the junction (t=130sec.)

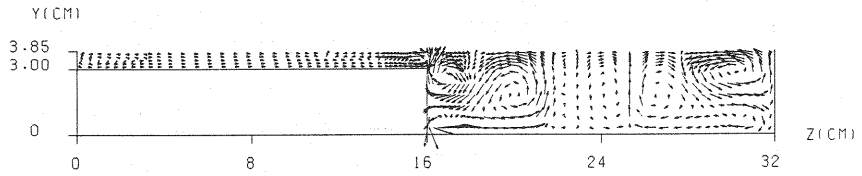

Fig.9 Spatially averaged flow patterns (t=130sec.)

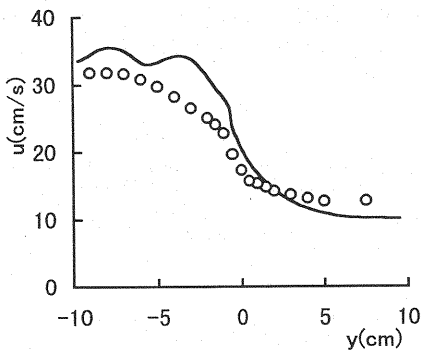

Fig.10 Transverse distribution of depth averaged velocity (Exp. and Cal.)

The cross-sectional flow pattern averaged spatially in the downstream part of the flume is shown in Fig.9. The upward flows around the central part of main channel, which was not observed in the previous experimental results (18), are induced in the figure, though the common secondary flow patterns are also reproduced near the corners of the cross section. Fig.10 shows the transverse distributions of depth-averaged velocity (stream-wise component).

Through the considerations of calculated results, it is indicated that the model refinement is needed to reproduce the 3-D flow structures and the secondary flow patterns more precisely.

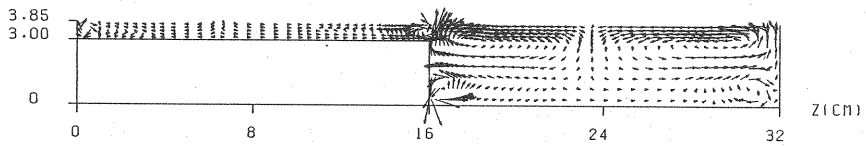

Fig.11 Spatially averaged flow patterns with the cubic terms

MODEL REFINEMENTS

To improve the model performance concerning the flow pattern of secondary currents, it is tested to include the cubic terms (3) given by Eq.11 in the constitutive equations 5 on trial.

$$\text{[the cubic terms]} = -C_4 \frac{k^2}{\varepsilon^2} D(\Omega_{ik}S_{kl}S_{lj} - S_{ik}S_{kl}\Omega_{lj})$$

$$-C_5 \frac{k^2}{\varepsilon^2} D(\Omega_{ik}\Omega_{kl}S_{lj} + S_{ik}\Omega_{kl}\Omega_{lj} - \frac{2}{3}S_{mn}\Omega_{no}\Omega_{om}\delta_{ij}) \qquad (10)$$

$$\Omega_{ij} = \frac{\partial U_i}{\partial x_j} - \frac{\partial U_j}{\partial x_i}$$

The numerical values of model constants, $C_4 = -0.03$ and $C_5 = 0$ are tested on trial. The cross sectional flow pattern is only calculated by using the large Δx, and is shown in Fig.11. The downward flows induced by the secondary currents can be seen around the central part of main channel, as indicated in the previous numerical and experimental studies (13,16,18), though further investigations are needed to verify the effect of the cubic terms on the Reynolds stresses and to tune the model constants.

CONCLUSIONS

The main results obtained in this study are summarized as follows:

(1) The computational model based on the non-linear $k-\varepsilon$ model with the quadratic terms and the effect of the strain parameter, S, on C_μ is tested to calculate the typical features of compound open channel flows. It is pointed out that the 3-D flow structures with both the horizontal vortices generated by the shear instability and the secondary currents of the second kind are reproduced qualitatively.

(2) To improve the model performance concerning the spatially averaged flow pattern of secondary currents, it is tested to include the cubic terms in the constitutive equations on trial. It is shown that the calculated results are improved qualitatively compared with the previous experimental studies, though the effect of cubic terms on the Reynolds stresses and the numerical values of model constants should be examined in detail.

REFERENCES

1. Fu, S., Rung, T. and Thiele F.: Realizability of non-linear stress-strain relationships for Reynolds-stress closures, Proc. of 11th Symposium on Turbulent Shear Flows, Grenoble, Vol.2, pp.13.1-13.6, 1997.

2. Fukuoka, S. And Fujita, K.: Prediction of flow resistance in compound channels and its application to design of river courses, J. Hydraulic, Coastal and Environmental Eng., JSCE, No.411/II-12, pp.63-72, 1989.
3. Gatski, T.B. and Speziale, C.G.: On explicit algebraic stress models for complex turbulent flows, J. Fluid Mech., Vol.254, pp.59-78, 1993.
4. Hirt, C.W. and Cook, J.L.: Calculating three dimensional flows around structures and over rough terrain, J. Computational Physics, Vol.10, pp.324-340, 1970.
5. Hosoda, T.: Turbulent diffusion mechanism in open channel flows, Ph D. Thesis, Kyoto University, 1990 (in Japanese).
6. Hosoda, T., Kimura, I. and Muramoto, Y.: Vortex formation processes in open channel flows with a side discharge by using the non-linear $k-\varepsilon$ model, Proc. of 11th Symposium on Turbulent Shear Flows, Grenoble, Vol.2, pp.19.1-19.6, 1997.
7. Ikeda, S., Murayama, N. and Kuga, T.: Stability of horizontal vortices in compound open channel flow and their 3-D structure, J. of Hydraulic, Coastal and Environmental Eng., No. 509/II-30, pp.131-142, 1995 (in Japanese).
8. Kato, M. and Launder, B.E.: The modeling of turbulent flow around stationary and vibrating square cylinders, Proc. 9th Symposium on Turbulent Shear Flows, Kyoto, Vol.1, pp.P10.4.1-10.4.6, 1993.
9. Kimura, I., Hosoda, T. and Muramoto, Y.: Numerical analysis of horizontal vortices in compound open channel flows by the two-layered flow model, Proc. of 27th Congress of IAHR, San Francisco, California, Vol. Theme A, pp.823-828, 1997.
10. Launder, B.E., Reece, G.J. and Rodi, W.: Progress in the development of a Reynolds-stress turbulence closure, J. Fluid Mech., Vol.68, pp.537-566, 1975.
11. Lin, B and Shiono, K.: Numerical modelling of solute transport in compound channel flows, J. of Hydraulic Research, Vol.33, No.6, pp.773-788, 1995.
12. Naot, D. and Rodi, W.: Calculation of secondary currents in channel flow, J. of Hydraulic Div., ASCE, 108(8), pp.948-968, 1982.
13. Naot, D., Nezu, I. and Nakagawa, A.: Hydrodynamic behaviour of compound rectangular open channel, J. of Hydraulic Engrg., ASCE, 119(3), pp.390-408, 1993.
14. Pezzinga, G.: Velocity distribution in compound channel flows by numerical modelling, J. of Hydraulic Engrg., ASCE, Vol.120, pp.1176-1198, 1994.
15. Pope, S.B. : A more general effective viscosity hypothesis, J. Fluid Mech., Vol.72, pp.331-340, 1975.
16. Sugiyama,H., Akiyama, M. and Matsubara,T.: Numerical simulation of compound open channel flow on turbulence with a Reynolds stress model, J. of Hydraulic, Coastal and Environmental Eng., No.515/II-31, pp.55-65, 1995 (in Japanese).
17. Tamai, N., Asaeda, T. and Ikeda, H.: Study on generation of personal large surface eddied in a composite channel flow, Water Resources Research, Vol.22, pp.1129-1138, 1986.
18. Tominaga,A. and Nezu,A.: Turbulent structure in compound open-channel flow, J. Hydraulic Eng., ASCE, Vol.117, No.1, pp.21-41, 1991.
19. Yoshizawa, A.: Statistical analysis of the deviation of the Reynolds stress from its eddy viscosity representation, Phys. Fluids, Vol.27, pp.1377-1387,1984.

APPENDIX – NOTATION

The following symbols are used in this paper:

A_1, A_2	= constants of non-linear k-ε model;
B	= constant used in Eq.9;
c_1, c_2	= constants of LRR model;
$C_1, C_2, C_3, C_4, C_5, C\mu$	= constants of non-linear k-ε model;
f_μ	= dumping function defined by Eq.9;
k	= turbulent energy;
p	= pressure;
S	= strain parameter defined by Eq.6;
S_{ij}	= components of strain rate tensors;
t	= time;
u_i	= components of turbulent velocity vectors;
U_i	= components of time averaged velocity vectors;
x_i	= spatial coordinates;
ε	= turbulent energy dissipation rate;
ν	= molecular dynamic viscosity.;
ρ	= density of fluid;
$\sigma_k, \sigma_\varepsilon$	= model constants of k-ε model;
Ω_{ij}	= components of rotation rate tensors.

(Received January 25, 1999 ; revised September 14, 1999)